

A Neural Network Controller New Methodology for the ATR-42 Morphing Wing Actuation

Abdallah Ben MOSBAH¹, Ruxandra Mihaela BOTEZ*¹, Thien My DAO²,
Mohamed Sadok GUEZGUEZ¹, Mahdi ZAAG¹

*Corresponding author

¹The Research Laboratory in Active Controls, Avionics and Aeroservoelasticity (LARCASE), Department of Automated Production Engineering, ETS, University of Quebec, Montreal, Que., Canada

abdallah.ben-mosbah.1@ens.etsmtl.ca, Ruxandra.Botez@etsmtl.ca*,
mohamed-sadok.guezguez.1@etsmtl.net, zaag.mahdi@gmail.com

²Department of Mechanical Engineering, ETS, University of Quebec, Montreal, Que., Canada
Thien-My.Dao@etsmtl.ca

DOI: 10.13111/2066-8201.2016.8.2.6

Received: 20 February 2016 / Accepted: 21 March 2016 / Published: June 2016

Copyright©2016. Published by INCAS. This is an open access article under the CC BY-NC-ND license (<http://creativecommons.org/licenses/by-nc-nd/4.0/>)

Abstract: A morphing wing model is used to improve aircraft performance. To obtain the desired airfoils, electrical actuators are used, which are installed inside of the wing to morph its upper surface in order to obtain its desired shape. In order to achieve this objective, a robust position controller is needed. In this research, a design and test validation of a controller based on neural networks is presented. This controller was composed by a position controller and a current controller to manage the current consumed by the electrical actuators to obtain its desired displacement. The model was tested and validated using simulation and experimental tests. The results obtained with the proposed controller were compared to the results given by the PID controller. Wind tunnel tests were conducted in the Price-Paidoussis Wind Tunnel at the LARCASE laboratory in order to calculate the pressure coefficient distribution on an ATR-42 morphing wing model for different flow conditions. The pressure coefficients obtained experimentally were compared with their numerical values given by XFOIL software.

Key Words: Neural networks, morphing wing, controller, electrical actuator modeling, wind tunnel

1. INTRODUCTION

To be able to design a morphing wing control system, it is essential to understand the motivation and the aerodynamic issues [1]. The fuel consumption can be reduced if the aerodynamic drag is reduced. An efficient way to reduce the drag is to develop a long laminar boundary layer by geometrical deformation of the airfoil in flight accordingly with flight conditions. The objective is to delay the flow transition on the upper surface of the wing [2]. The “morphing” is done with the aim to change one or more parts of a structure geometry in order to improve its aerodynamic performances [4]. Accordingly to Sofla *et al.* [5], “morphing” can be achieved to change the geometry along the chord, the span or the camber of the airplane wing to improve the lift and reduce the drag. The determination of the

appropriate airfoil for each flight case was done for an optimization phase by means of experimental flight tests or using optimization algorithm [6]. Campanile and Sachau [7] proposed a method to modify the camber of the wing. Another concept was used by Chandrasekhara *et al.* [8] to adapt the leading edge, while Hetrick *et al.* [9] presented a compliant structure to change the geometry of the wing trailing edge. Many other morphing wing studies have been proposed to improve the lift [10, 11, 12], or to obtain a better laminarity of the flow [13, 14]. A numerical model based on a genetic algorithm was used by Strelec *et al.* [15] to optimize the shape parameters of an airfoil. For the use of an experimental optimization method, Hetrick *et al.* [9] proposed an approach to determine the optimal flap deflections. A genetic algorithm was used by Boria *et al.* [16] to optimize a unmanned morphing wing and to test it in a Wind Tunnel. Their proposed model aimed to maximize the lift and efficiency by using a wind tunnel [16]. A multidisciplinary approach was proposed by Sainmont *et al.* [17] to change the morphing upper surface and to optimize the laminar airfoil. For the deformation of the wing skin, the use of a reliable and accurate actuation and control system is necessary to obtain the desired shape determined in the optimization phase. A closed-loop control system was proposed by Popov *et al.* [18, 19] to validate a morphing wing model in a wind tunnel. Another study based on using an open-loop controller to test a morphing wing was presented by Popov *et al.* [20]. The same authors presented the optimization of a morphing wing in real time using wind tunnel validation tests [21]. Grigorie *et al.* [22 to 25] have proposed many controllers based on different techniques; in [22, 23] they proposed a new control technique using a combined PI and bi-positional laws optimum for a morphing wing application. An actuation mechanism and a control technique based on on-off proportional-integral-controllers were proposed and tested experimentally [24, 25]. Many other control methods are used extensively in the literature, such as Fuzzy Logic and Neural Networks (NN). These two methods are also used, alone or in hybridization, to resolve many other problems, such as classification, optimal control and manufacturing [26]- [30]. These methods are extremely efficient to solve nonlinear and multidimensional systems. Xuan *et al.* [31] proposed a controller of uncertain parameters for nonlinear systems based on NN and Fuzzy Logic methods. Botez *et al.* [32] have explained in details the content of the CRIAQ Project 7.1 regarding the design and manufacturing of a morphing wing equipped with smart material actuators and pressure sensors with the aim to delay the transition of the flow on the wing, and therefore to improve the aerodynamic performance of the wing. Mamou *et al.* [33] have presented a summary of the results obtained in the CRIAQ project 7.1, where CRIAQ is the abbreviation of the ‘Consortium for Research and Innovation in Aerospace in Quebec’. A hybrid fuzzy logic proportional-integral-derivative and a conventional on-off controller were proposed by Grigorie *et al.* [34, 35] for morphing wing actuation. Two other control applications based on Fuzzy Logic were proposed by the same authors [36, 37]. Rosario *et al.*, [38]- [41] have developed structural and aeroelastic analyses for morphing wing flap design, while Barbarino *et al.* [42] have presented numerical and experimental methodologies and results for airfoil structural morphing studies equipped with smart material actuators. Large complex problems in aerospace engineering have been solved using NNs. Rauch *et al.* [43] used NNs to implement fault detection in aircraft. Models based on NNs techniques are proposed by Linse and Stengel [44], Wallach *et al.* [45] and Mosbah *et al.* [46, 47, 48] to identify and predict aerodynamic coefficients, and other methods for detection and icing identification were developed in [49, 50, 51]. Controllers for autopilot systems based on NNs were developed by Napolitano and Kincheloe [52]. Mosbah *et al.* [53] developed a new hybridization NNs model and extended the great deluge algorithm; their model was validated

using wind tunnel test. In this study, a control system based on NNs is proposed. The model is designed to be incorporated in a morphing wing model used and validated experimentally during wind tunnel testing.

2. ATR-42 MORPHING WING MODEL

A mechanism was developed in order to build an experimental prototype of a morphing model which will be used in wind tunnel tests. This mechanism consists principally of two eccentric axes mounted inside the model and animated in rotation by two electric actuators. The system is used to change the upper surface of the model using the eccentric axes; moved by its rotation, the axes push the composite skin vertically upwards at 30% and 50% of the chord to obtain the desired deformation of up to 4 mm. The required amount of force that needs to be developed by each actuator line on the skin to produce the desired deformation mainly depends on the composite structure of the skin, including the positions and the number of the actuators. Coutu *et al.* [6] demonstrated that two actuation rows were sufficient to obtain good aerodynamic results for a morphing wing skin equipped with SMAs [1]. Figure 1 shows the ATR-42 morphing wing model assembled with the deformation skin mechanism and Figure 2 shows the airfoil of the ATR-42 wing model and the position of the eccentric axes.

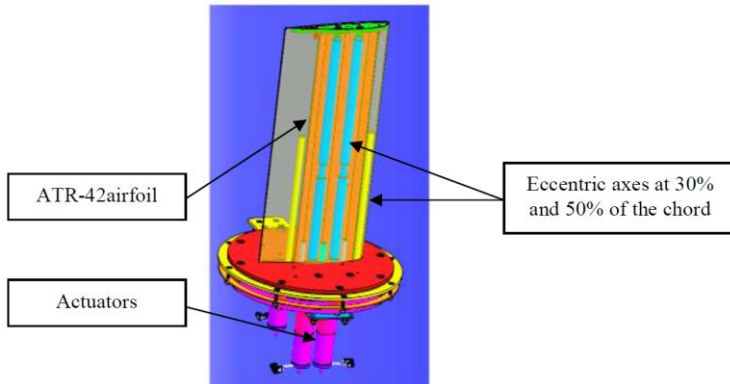


Figure 1. CAD of the ATR-42 model

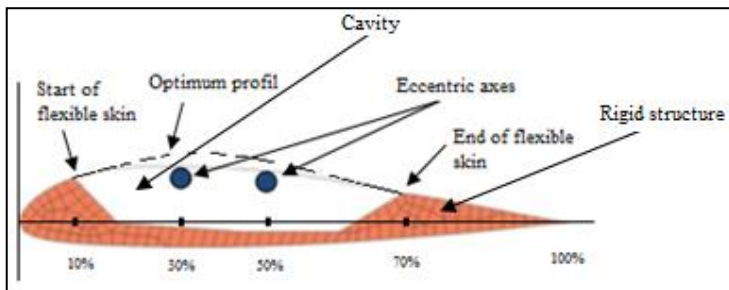


Figure 2. ATR-42 airfoil

3. THE CLOSED LOOP ARCHITECTURE OF THE MODEL

To obtain the desired airfoil shape, we need to deform the skin using two actuators. These deformations should be as close as possible (equal) experimentally with those determined numerically; a robust position controller is needed. The two actuators that deform the airfoil

of the model from its original to its desired shape and the architecture of the control scheme are shown in Figure 3.

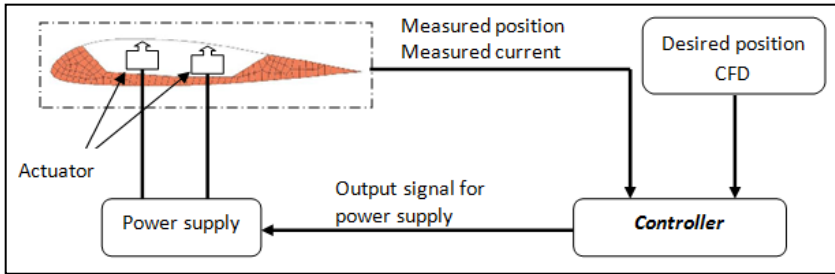


Figure 3. Architecture of the closed loop system control

3.1 Controller architecture

As shown in Figure 4, the control system is composed of a position controller, a current controller, a saturation voltage block to protect the motor, and a DC motor block.

A control system based on the Proportional Integral Derivative PID was proposed by Kammegne *et al.* [3] to control the actuators positions of the ATR-42 morphing wing model (the same model used in this study). The results obtained with the PID controller were satisfactory, with an error margin of 0.4 %. The concept here is to replace the PID controller with another controller based on neural networks, for more precision and comparison purposes between the efficiencies of both controllers. The “*position controller*” bloc and the “*current controller*” bloc shown in Figure 4 are replaced by two NN blocs obtained by the proposed algorithm.

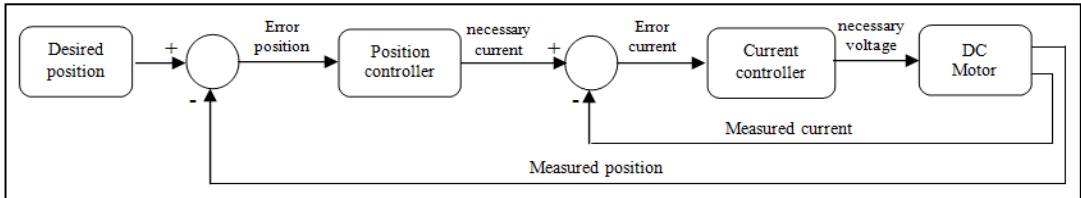


Figure 4. Closed loop control

3.2 Modeling of the DC motor

The deformation of the skin is realized using two DC motors, and in order to obtain the exact desired deformation, a robust control system should be used. Firstly, the mathematical model of the motors is identified. The DC motors can be configured using electrical, electromechanical and mechanical engineering equations [1]. Figure 4 represents the DC motors’ armature.

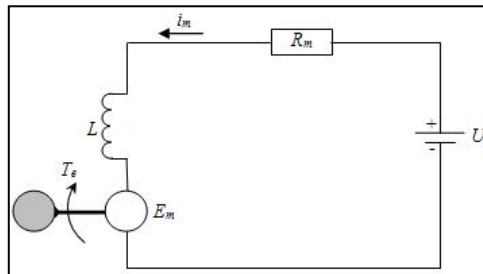


Figure 5. Representation of the DC motors

where:

U – voltage [V], R_m – resistance [Ω], L – inductance [H], i_m – current [A],
 T_e – torque [$\text{N}\cdot\text{m}$], E_m – counter-electromotive force.

As described by Jérémy [1] and Kammegne et al. [3], the motor resistance R_m and the inductance are assumed to be constants. The actuator model can be described by the following equations:

$$U = R_m i_m + L \frac{di_m}{dt} + E_m \quad (1)$$

$$E_m = k_e W_m \quad (2)$$

$$T_e = k_t i_m \quad (3)$$

$$T_e = k_f W_m + J \frac{dW_m}{dt} + T_L \quad (4)$$

where:

W_m – motor angular speed [rad/s], k_e – angular speed constant [revolution/min/V],
 k_f – friction coefficient [$\text{N}\cdot\text{m}/(\text{rad}/\text{s})$], T_L – load torque [$\text{N}\cdot\text{m}$], J – inertia [$\text{Kg}\cdot\text{m}^2$].

To study the stability of a real system such as that of a DC motor, a Laplace transform must be applied to switch from the time domain to the frequency domain. The Laplace transform of equation (1) is the following:

$$U(S) = R_m \cdot I_m(S) + L \cdot S \cdot I_m(S) + k_e \cdot W_m(S) \quad (5)$$

$$I_m(S) = \frac{U(S) - k_e \cdot W_m(S)}{R_m + L \cdot S} \quad (6)$$

and the Laplace transform of equation (4) is:

$$T_e(S) - T_L(S) = k_f \cdot W_m(S) + J \cdot S \cdot W_m(S) \quad (7)$$

From where:

$$W_m(S) = \frac{T_e(S) - T_L(S)}{k_f + J \cdot S} \quad (8)$$

and by replacing the Laplace transform of equation (3) into equation (8), we obtain:

$$W_m(s) = \frac{k_t}{k_f + J \cdot S} \cdot I_m(S) - \frac{T_L(S)}{k_f + J \cdot S} \quad (9)$$

where “S” is the Laplace operator.

In the absence of the load torque, i.e., $T_L=0$, by replacing $T_L=0$ into equation (9), the $I_m(s)$ can be written as follows:

$$I_m(s) = \frac{J \cdot s + k_f}{k_t} W_m(s) \quad (10)$$

By replacing $I_m(S)$ given by equation (10) in equation (5), the motor voltage $U(S)$ becomes:

$$U(s) = (L \cdot s + R_m) \frac{J \cdot s + k_f}{k_t} W_m(s) + k_e \cdot W_m(s) \quad (11)$$

The transfer function of the model, by use of equations (9) and (11), is:

$$G(s) = \frac{W_m(s)}{U(s)} = \frac{k_t}{J \cdot L \cdot s^2 + (R_m \cdot J + k_f \cdot L) \cdot s + k_f \cdot R_m + k_e \cdot k_t} \tag{12}$$

In our morphing wing model of the ATR-42, a *Maxon* motor is used. The datasheet provided by the manufacturer includes the internal motor characteristics to calculate the modeling parameters. These characteristics are presented in Table 1.

Table 1. Internal Motor Characteristics

R_m [Ω]	J [$\text{kg}\cdot\text{m}^2$]	K_t [Nm/A]	L [H]	K_f [$\text{Pa}\cdot\text{s}$]
11.4	65.9e-7	0.119	0.0316	1.01738 · 10 ⁻⁵

The model has been validated by Brossard, J. [1] and Kammegne *et al.* [3]; its validation consisted in the comparison of the values of i_m and w_m given by the manufacturer with simulation values using Matlab/ Simulink. The results confirmed that the model was working well. The obtained values of the motor current and the motor speed were the same as the values given by the manufacturer.

4. NEURAL NETWORK CONTROL SYSTEM DESIGN

To design a robust control system, a position controller and a current controller are needed, as seen in Figure 4. These two blocs have a very good performance in order to obtain good results from the control system. Two Neural Networks are designed to ensure a high performance level. The first NN is used to control the position, for which where the inputs are the desired positions in degrees and the output is the needed current. The second neural network controller is used to control the current consumed by the motor; the input of this bloc is the current and the output is the voltage required to reach the desired position. Figure 6 shows the architecture of our control system, using 2 NN algorithms.

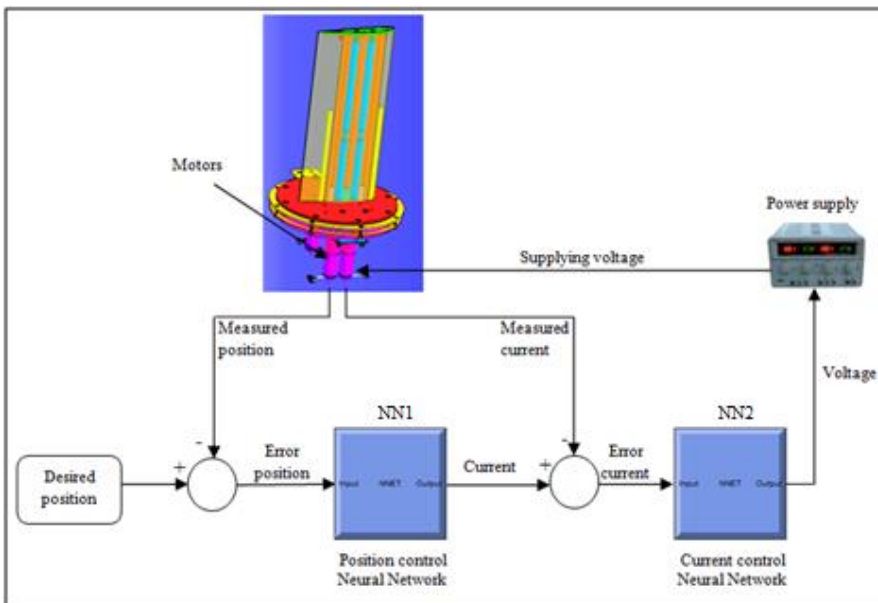


Figure 6. Control system architecture

Each neural network controller of the “*position controller*” and the “*current controller*”, needs a database. The motor used here works using a current between -3.5A and 3.5A and a voltage of -48V to 48V. The database for the first NN controller is composed of the desired position in degrees, and the current for which this position represents the input and the current represents the output. This database is used to train the neural network, therefore it can be used to control the current values. The output of the first neural network (the position controller) is the input of the second (the current controller), as seen on Figure 6. For the training phase of the second neural network, the selected database is composed of the current values as an input of the current controller, and the output is the voltage value supplied to the power supply, then to the motor to obtain the desired deformation. The challenge of this methodology resides in the choice of two databases to obtain the desired deformation of the morphing wing. The idea is to accelerate the system when errors are important at the beginning of the simulation and avoid overshooting. Tests are needed to determine the proper data. The training started using linear inputs and outputs. For the first controller, the inputs values are the error between the desired position and the measured position (-360° to 360° with step equal to 0.18), and the outputs are the current between -3.5A to 3.5A with step equal to $1.75 \cdot 10^{-3}$. We need to accelerate the system when the measured value is very far from the desired value. For the second controller, the inputs values are the current between -3.5A and 3.5A with step equal to 0.01 and the outputs are the voltages between -48V to 48V with step equal to -0.137. For this objective, different data are tested and the results are analyzed to define the right interval. Following a few number of tests, we were able to construct databases that gave good results. Tables 2 and 3 represent the databases used to train the neural network position controller (Table 2 and Figure 7), and the database used to train the neural network current controller (Table 3 and Figure 8), respectively. In Table 2, for the values of deformations between -360° and -50° , in order to accelerate the system, the output current is fixed at -3.5A, while for the deformation values between 50° and 360° , the intensity of the current is equal to 3.5A. For the deformation values between -50° and 50° , the intensity of the current varies between -3.5A and 3.5A as described by the following equation $Current=0.07*position$, and as shown in Figure 7.

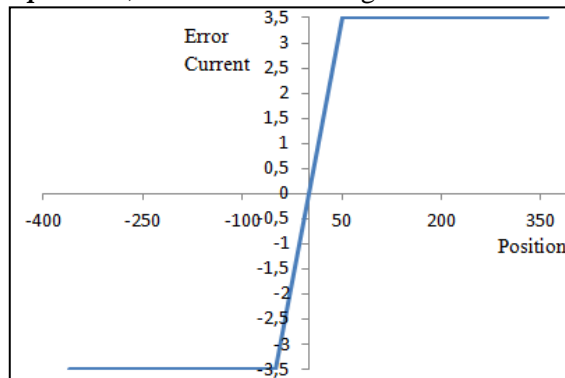


Figure 7. Used data to train the position controller

Table 2. “Position controller” database

The input: the deformation [degree]	The output: the current [A]
$-360 \text{ degree} < \text{deformation} < -50 \text{ degrees}$	-3.5 A
$-50 \text{ degree} \leq \text{deformation} \leq 50 \text{ degrees}$	$0.07 * \text{deformation}$
$50 \text{ degree} < \text{deformation} < 360 \text{ degrees}$	3.5 A

In Table 3, for the current values between - 3.5A and - 0.6A, the output voltage value is -48V and for the current values between 0.6A and 3.5A, the corresponding voltage is equal to 48V. For the range of current values between -0.6A and 0.6A, the output voltage varies between -48V and 48V as given by the following equation **Voltage = 80*current**, and as shown in Figure 8.

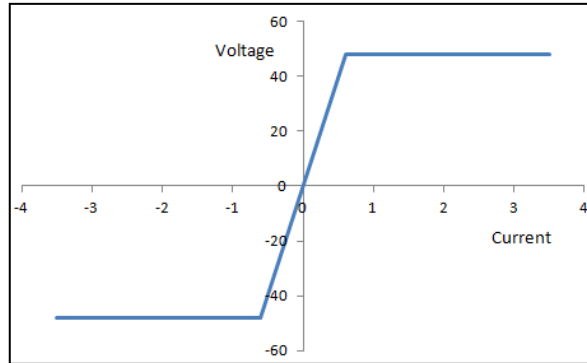


Figure 8. Used data to train the current controller

Table 3. “Current controller” database

The input: the current [A]	The output: the voltage[V]
$-3.5 < \text{current} < -0.6$ A	-48 V
$-0.6 \text{ A} \leq \text{current} \leq 0.6$ A	$80 \times \text{current}$
$0.6 \text{ A} < \text{current} < 3.5$ A	48 V

Using the databases shown in Tables 2 and 3, the Neural Networks are designed using the following method:

- Step 1: Initialization of the neural network, number of layers = 1;
- Step 2: Randomly selection of the number of neurons between 1 and 15;
- Step 3: Training using error= 10^{-4} ; and
- Step 4: If the training error is not reached, then the layer number = layer number +1 and go to step 1.

The first NNs’ position controller is composed of 3 layers of 14, 13 and 14 neurons, and 1 output layer of 1 neuron (Figure 9). The second controller is composed of 2 layers of 14 and 9 neurons, its output layer is composed of one neuron (Figure 10). The non-linear transfer function used in the proposed models is “Logarithmic sigmoid”; the transfer function of the output layer is linear.

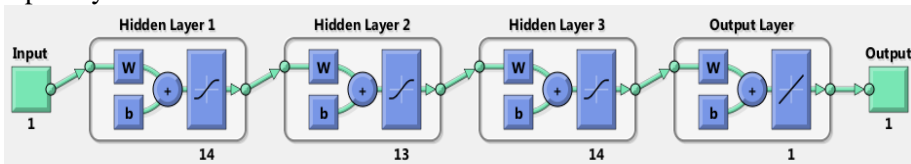


Figure 9. NNs’ Architecture of the Position Controller

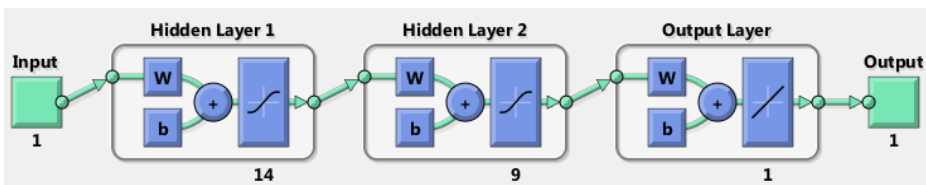


Figure 10. NNs’ Architecture of the Current Controller

Let $Output^{(k)}$ represent the outputs of layer k , so that the general formula to calculate the outputs $Output^{(k)}$ is the following:

$$Output_j^{(k)} = \text{tansig} \left(\sum_{i=1}^n Output_i^{(k-1)} \times w_{i,j} + b_j \right) \quad (13)$$

where j is the index of neurons in the layer (k), n is the number of the neurons in the layer ($k-1$), and i is the index of neurons in the layer ($k-1$).

The proposed controller is further compared to the PID controller developed in [3]. The simulation results using Matlab/ Simulink allow the comparison between the performance of the NNs' controller with that of the PID controller.

The error obtained by the PID controller is close to 0.4 %, while the NNs controller gives the exact desired values, as shown in Figure 11.

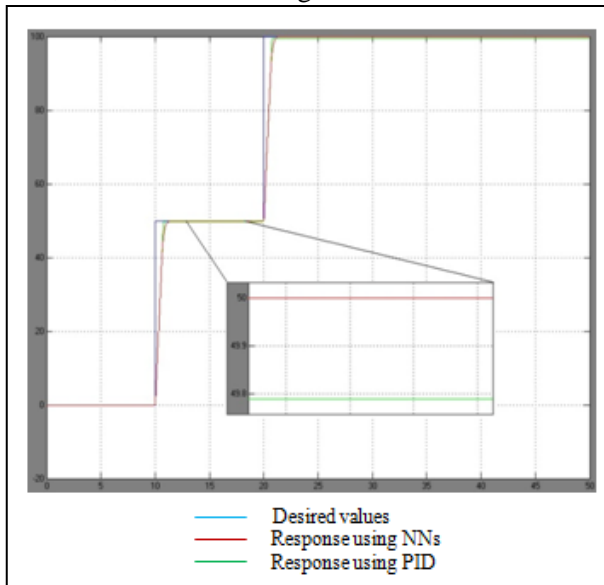


Figure 11. Response Position using PID versus NNs (degree/time (s))

5. EXPERIMENTAL WORK

5.1 Concept of the Experimental Work

In order to validate the performance of the controller obtained during its simulation, a HIL (Hardware in the Loop) process is used which implements the controller simulation via the Labview real time environment.

Labview offers not only the possibility to communicate in real time with the different components of our hardware loop, it also allows control algorithms and model simulations to be imported from other modeling environments through the model interface toolkit, thus, this Labview interface enables the interaction between Labview and third-party modeling environments. The validation concept, shown in Figure 12, is based on the idea of establishing communication channels between the hardware components, and the Simulink controller. The Labview program ensures that all the data required for their control operations can be read, processed and sent to a controller. This controller will generate the

correct control signal based on the external command from the operator. The type of signals and the order of the operations are described in the following sections.

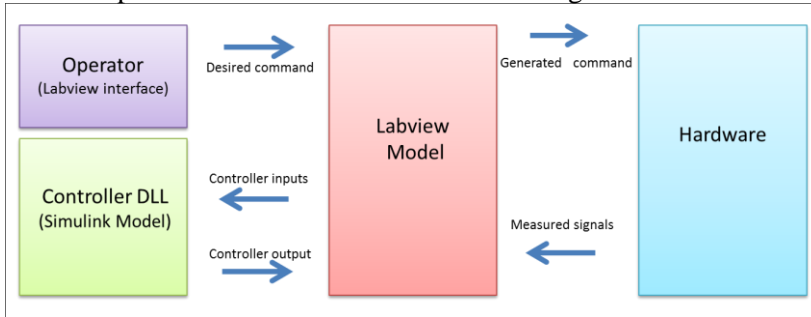


Figure 12. Validation Concept

5.2 Experimentation and Real Time Validation

After finding the correct controller for the simulation, we need to prepare it for real-time testing. The target platform in our case is Windows.

5.2.1 Hardware

The hardware used for testing and validation is specified in Table 4:

Table 4. List of the hardware used in the experiment

<i>Hardware</i>	<i>Characteristics</i>
Motor	Maxon motor : RE 35 Ø35 mm, Graphite Brushes, 90 Watt
Gear box	Planetary Gearhead GP 32 HP Ø32 mm, 4.0 - 8.0 Nm
Encoder	Encoder MR, Type L, 512 CPT, 3 Channels, with Line Driver
Drive	EPOS2 24/5, Digital positioning controller, 5 A, 11 - 24 VDC
Power supply	CPX400DP- programmable dual output 2 x 420 watts

The wiring and installation are specified in Figure 11:

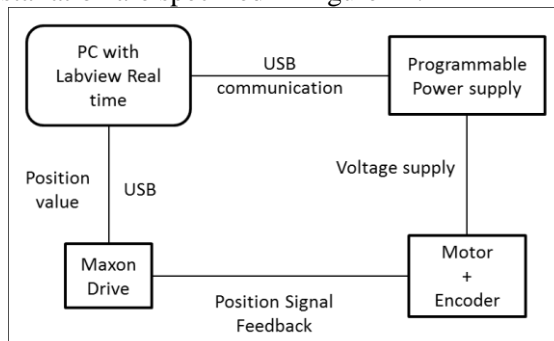


Figure 13. Hardware Installation

The “Windows Host” communicates using USB with the programmable power supply and the drive *Maxon*, this drive is used to read and process the angle position value returned by the encoder on the motor. The DC motor is fed directly through the power supply, as seen in Figure 13.

5.2.2 Real-Time Model

First of all, the input and output ports of the controller are created as shown in Figure 14; the controller will need the desired position (input 1), the position feedback (input 3), and the

current feedback (input 2). Regarding the configuration parameters of the Matlab/Simulink model, the solver needs to be “discrete” and the “step solver” should be chosen as a “fixed step” with a size of five millisecond (5 msec). The system target file should be ‘NIVERistand.tlc’ in order to be used with Labview in real time.

After desired form of the controller has been given the, and the configurations parameters have been set as mentioned above, the model can be built using Matlab’s Real-Time Workshop. The Labview model’s function is to ensure the interface and the data exchange between the hardware and the controller.

Using the CPX400 DP library in Labview, a USB communication channel is established with the power supply; through this channel, we are able to perform some actions such as opening a session, initializing a device, enabling/ disabling the output, settling the voltage value and reading the average current value.

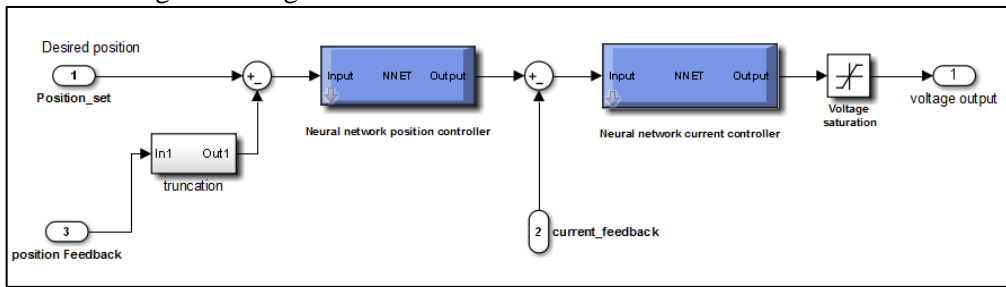


Figure 14. Simulink / Labview Real-Time Model

For the calculations of position values, the *Maxon* drive is used to read and process the encoder signal and return the exact angle; some operations are needed to obtain their values in degrees.

The Labview program will need to load the controller model as a Dynamic Link Library (DLL), which would be generated during the preparation step when building the Matlab Simulink model. This task is performed using the Model Interface Toolkit VIs by specifying the path of the generated DLL in order to load it, and by obtaining the sampling time.

5.2.3 Validation Results

A step of 50° and another of 100° were sent to the motor in order to test the performance of the implemented controller (Figure 15). The results obtained are very good; the error for 50° is equal to 0%, while the error for 100° , is equal to 1%.

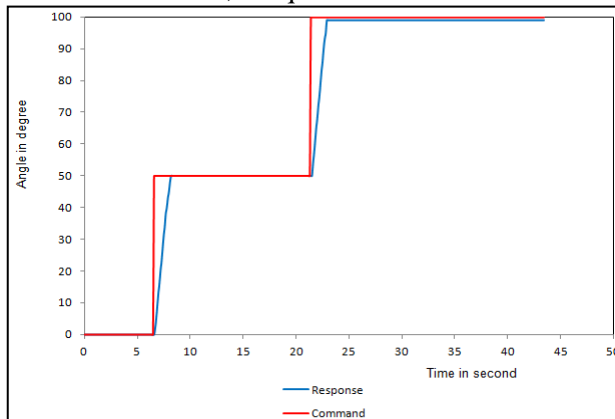


Figure 15. Experimental Results

5.3 Wind Tunnel Tests

The experimental results achieved by using the Price-Paidoussis blow down wind tunnel are presented here. The pressure on the morphing surface of an ATR-42 wing is measured using a pressure transducer to determine the pressure coefficient distribution (C_p). The experimental results are compared with numerical values obtained using XFOIL code.

5.3.1 Experimental Tests Equipment

The Price-Paidoussis wind tunnel and the pressure transducer system are presented here. The experiment was done using the Price-Paidoussis subsonic wind tunnel at the Research Laboratory in Active Controls, Avionics and Aeroservoelasticity (LARCASE). The Price-Paidoussis wind tunnel is presented in Figure 16. This subsonic wind tunnel is equipped with two test chambers; the first provides a maximum airspeed of 60 m/s and the second offers a maximum airspeed of 40 m/s.



Figure 16. Price-Paidoussis Wind Tunnel

The measurement system was the *Multitube Manometer tubes* system, as its name indicates, this system is equipped with thirty-six tube tilting manometers to measure pressures taken from pressure taps on the ATR-42 morphing wing model (Figure 17) in the Price-Paidoussis subsonic wind tunnel. The tubes are filled with colored water to obtain very good visibility for the readings. The *Multitube Manometer tubes* transducer is shown in Figure 18.



Figure 17. ATR-42 Morphing Wing Model



Figure 18. Multitube Manometer Transducer

5.3.2 Experimental Results

This section presents the results obtained at the LARCASE laboratory using the Price-Paidoussis subsonic wind tunnel. The locations of the pressure taps along the chord on the morphing surface of the ATR-42 wing airfoil are indicated in Table 5.

Table 5. Location of pressure taps

Pressure taps number	1	2	3	4	5	6	7	8	8	9	11	12	13	14
Position (%of the chord)	5	10	15	20	25	30	32.5	35	37.5	40	45	50	60	70

Three flight cases were considered during the wind tunnel tests. These tests were conducted for three different angles of attack (-2° , 0° and 2°) and one Mach number equal to 0.08 (34 m/s). The experimental results are compared with results given by XFOIL code. As shown in Figures 19 to 21, the experimental pressure coefficients C_p are in a very good agreement with the theoretical pressure coefficients results obtained using XFOIL code.

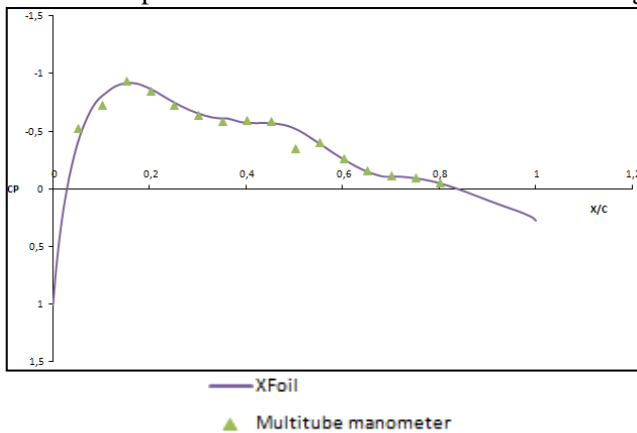


Figure 19. Experimental results (multitube manometer) of pressure coefficients C_p is for the angle of attack $\alpha=0^\circ$ and Mach number=0.08

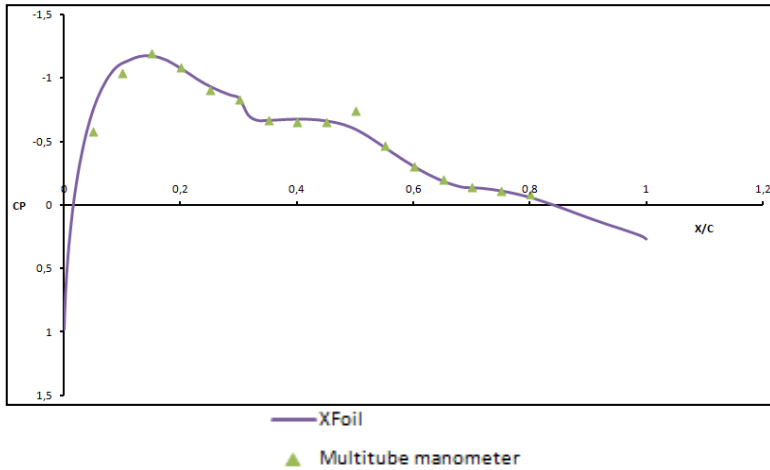


Figure 20. Experimental results (*multitube manometer*) of pressure coefficients C_p is for the angle of attack $\alpha=2^\circ$ and Mach number=0.08

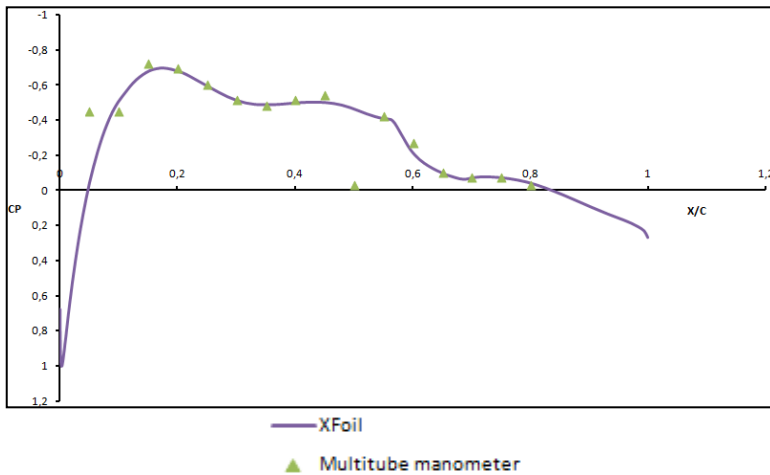


Figure 21. Experimental results (*multitube manometer*) of pressure coefficients C_p is for the angle of attack $\alpha=-2^\circ$ and Mach number=0.08

6. CONCLUSION

In this paper, a NN controller was designed and tested for an ATR-42 morphing wing. The objective is to reproduce a desired specific shape of the morphing wing using electric actuators. A robust controller is necessary to obtain a very good precision in order to achieve the exact desired airfoil shape. The proposed NN algorithm is used for a new closed loop controller methodology. The NN models are designed using Matlab and are further converted into Simulink model to be used for a closed loop controller methodology. The simulation gave very good results; the model's responses give the desired values. The model is compared to a PID controller. The NN controller gives a more accurate performance than the PID controller; during experimental tests, it gave very precise results. The pressure coefficients obtained using wind tunnel tests are compared with the pressure coefficients given by XFOIL software, and confirm the obtainment of a very good performance level.

ACKNOWLEDGMENTS

Many thanks are due to Professors Michael Païdoussis and Stuart Price for the donation of their Subsonic Blow Down Wind Tunnel to the LARCASE laboratory at ETS headed by Professor Ruxandra Mihaela Botez. Special thanks are due also to Mr Oscar Carranza Moyao and to Mrs Odette Lacasse from ETS.

This research was financially supported by the Natural Sciences and Engineering Research Council of Canada (NSERC) in the Canada Research Chair in Aircraft Modeling and Simulation Technologies Program.

REFERENCES

- [1] J. Brossard, *Closed loop control on morphing wing in the Price-Païdoussis wind tunnel*, Master Thesis, École de technologie supérieure, Université du Québec, Montréal, Qué., Canada, 2013.
- [2] A. Koreanschi, O. Sugar Gabor, R. Botez, *New Numerical Study of Boundary Layer Behavior on A Morphing Wing-with-Aileron System*, AIAA's Aviation 2014, 32nd Applied Aerodynamics Conference, Atlanta, GA, USA, 16 - 20 June, 2014.
- [3] M. J. Kammegne Tchatchueng, L. T. Grigorie, R. M. Botez, A. Koreanschi, *Design and validation of a position controller in the Price-Païdoussis wind tunnel*, IASTED Modeling, Simulation and Control Conference, Innsbruck, Austria, 17-19 February, 2014.
- [4] T. A. Weisshaar, *Morphing aircraft technology-new shapes for aircraft design*, DTIC Document, NATO Conference, 2006.
- [5] A. Y. N Sofla, S. A. Meguid, K. T. Tan, W. K. Yeo, Shape morphing of aircraft wing: Status and challenges, *Materials & Design*, vol. **31**, no 3, pp. 1284-1292, 2010.
- [6] D. Coutu, *Design and operation of an active structure for an experimental morphing laminar wing*, PhD Thesis, École de technologie supérieure, Montreal, Que., Canada, 2010.
- [7] L. F. Campanile, D. Sachau, The belt-rib concept: a structronic approach to variable camber, *Journal of Intelligent Material Systems and Structures*, **11**(3), pp. 215-24, 2000.
- [8] M. S. Chandrasekhara, L. W. Carr, M. C. Wilder, M. C. Paulson, C. D. Sticht, *Design and development of a dynamically deforming leading edge airfoil for unsteady flow control*, Proceedings of the 17th IEEE International Congress on Instrumentation in Aerospace Simulation Facilities, Piscataway, USA, pp. 132-140, 1997.
- [9] J. A. Hetrick, R. F. Osborn, S. Kota, P. M. Flick, D. B. Paul, *Flight testing of Mission Adaptive Compliant Wing*, Structural Dynamics, and Materials Conference, Waikiki, HI, USA, April 23-27, p. 92-109, 2007.
- [10] A. Baron, B. Benedict, N. Branchaw, B. Ostry, J. Pearsall G. Perlman J. Selstrom, *Morphing Wing (MoW)*, Department of Aerospace Engineering, Rept. ASEN 4018, University of Colorado at Boulder, CO., USA, 2003.
- [11] S.-M. Yang, J.-H. Han, I. Lee, Characteristics of smart composite wing with SMA actuators and optical fiber sensors, *The International Journal of Applied Electromagnetics and Mechanics*, **23** (3-4), pp. 177-186, 2006.
- [12] J. K. Strelec, D. C. Lagoudas, M. A. Khan, J. Yen, Design and implementation of a shape memory alloy actuated reconfigurable airfoil, *Journal of Intelligent Material Systems and Structures*, Vol. **14** (4-5), pp. 257-273, 2003.
- [13] D. Munday, J. Jacob, *Active control of separation on a wing with conformal camber*, 39th AIAA Aerospace Sciences Meeting and Exhibit, Reno, Nevada, USA, 8-11 January, 2001.
- [14] A. L. Martins, F.M. Catalano, *Aerodynamic optimization study of a mission adaptive wing for transport aircraft*, 15th AIAA Applied Aerodynamics Conference, Atlanta, GA, USA, pp. 471-480, 23-25 June, 1997.
- [15] J. K. Strelec, D. C. Lagoudas, M. A. Khan, J. Yen, Design and implementation of a shape memory alloy actuated reconfigurable airfoil, *Journal of Intelligent Material Systems and Structures*, Vol. **14**, no. 4-5, pp. 257-273, 2003.
- [16] F. Boria, B. Stanford, P. Ifju, Evolutionary Optimization of a Morphing Wing with Wind-Tunnel Hardware in the Loop, *AIAA Journal*, Vol. **47**, No. 2, pp. 399-409, 2009.
- [17] C. Sainmont, I. Paraschivoiu, D. Coutu, *Multidisciplinary Approach for the Optimization of a Laminar Airfoil Equipped with a Morphing Upper Surface*, Symposium on Morphing Vehicles, NATO VT-168, Evora, Portugal, 2009.

- [18] A. V. Popov, T. L. Grigorie, R. M. Botez, M. Mamou, Y. Mébarki, Closed-Loop Control Validation of a Morphing Wing Using Wind Tunnel Tests, *Journal of Aircraft*, Vol. **47**, No. 4, pp. 1309-1317, 2010.
- [19] A. V. Popov, M. Labib, J. Fays, R. M. Botez, Closed loop control simulations on a morphing laminar airfoil using shape memory alloys actuators, *AIAA Journal of Aircraft*, Vol. **45**, No. 5, pp. 1794-1803, 2008.
- [20] A. V. Popov, T. L. Grigorie, R. M. Botez, Y. Mébarki, M. Mamou, Modeling and testing of a morphing wing in open-loop architecture, *AIAA Journal of Aircraft*, Vol. **47**, No. 3, pp. 917-923, 2010.
- [21] A. V. Popov, T. L. Grigorie, R. M. Botez, M. Mamou, Y. Mébarki, Real Time Morphing Wing Optimization Validation Using Wind-Tunnel Tests, *AIAA Journal of Aircraft*, Vol. **47**, No. 4, pp. 1346-1355, 2010.
- [22] T. L. Grigorie, A. V. Popov, R. M. Botez, M. Mamou, Y. Mébarki, *A morphing wing used shape memory alloy actuators new control technique with bi-positional and PI laws optimum combination. Part 1: design phase*, 7th International Conference on Informatics in Control, Automation and Robotics ICINCO 2010, 15-18 June, Funchal, Madeira, Portugal, 2010.
- [23] T. L. Grigorie, A. V. Popov, R. M. Botez, M. Mamou, Y. Mébarki, *A morphing wing used shape memory alloy actuators new control technique with bi-positional and PI laws optimum combination. Part 2: experimental validation*, 7th International Conference on Informatics in Control, Automation and Robotics ICINCO 2010, 15-18 June, Funchal, Madeira, Portugal, 2010.
- [24] T. L. Grigorie, A. V. Popov, R. M. Botez, M. Mamou, Y. Mébarki, On-off proportional-integral-controller for a morphing wing. Part 1: Actuation mechanism and control design, Proceedings of the Institution of Mechanical Engineers, Part G, *Journal of Aerospace Engineering*, vol. **226**, no 2, pp. 131-145, 2012.
- [25] T. L. Grigorie, A. V. Popov, R. M. Botez, M. Mamou, Y. Mébarki, On-off proportional-integral-controller for a morphing wing. Part 2: Control validation-numerical simulations and experimental tests, Proceedings of the Institution of Mechanical Engineers, Part G, *Journal of Aerospace Engineering*, vol. **226**, no 2, pp. 146-162, 2012.
- [26] B. K. Wrong, S. L. Vincent, J. Lam, A bibliography of neural network business applications research: 1994–1998, *Computers and Operation Research*, Vol. **27**, pp. 1045–1076, 2002.
- [27] K. J. Hunt, D. Sbarbaro, R. Zbikowski, P. J. Gawthrop, Neural networks for control systems – a survey, *Automatica*, Vol. **28**, pp. 1083–1112, 1992.
- [28] G. J. Udo, Neural networks application in manufacturing process, *Computers and Industrial Engineering*, Vol. **23** (1–4), pp. 97–100, 1992.
- [29] B. K. Wong, T. A. Bodnovich, Y. Selvi, Neural network application in business: a review and analysis of the literature (1988–1995), *Decision Support Systems*, Vol. **19**, pp. 301–320, 1997.
- [30] D. Chen and P. Burrell, On the optimal structure design of multilayer feedforward neural networks for pattern recognition, *International Journal of Pattern Recognition and Artificial Intelligence*, Vol. **6** (4), pp. 375–398, 2002.
- [31] C.-Z. Xuan, Z. Chen, P. Wu, Y. Zhang, W. Guo, *Study of fuzzy neural network on wind velocity control of low-speed wind tunnel*, International Conference on Electrical and Control Engineering, 2010.
- [32] R. M. Botez, P. Molaret, E. Laurendeau, *Laminar Flow Control on a Research Wing – Project Presentation on a Three-Year Period*, Canadian Aeronautical Society Institute CASI Aircraft Design and Development Conference, Toronto, Ont., Canada, April 25-26, 2007.
- [33] M. Mamou, Y. Mébarki, M. Khalid, M. Genest, D. Coutu, A. V. Popov, C. Sainmont, T. Georges, L. T. Grigorie, R. M. Botez, V. Brailovski, P. Terriault, I. Paraschivoiu, E. Laurendeau, *Aerodynamic Performance Optimisation of a Wind Tunnel Morphing Wing Model subject to various cruise flow conditions*, 27th International Congress of the Aeronautical Sciences ICAST 2010, Nice, France.
- [34] T. L. Grigorie, R. M. Botez, A.V. Popov, M. Mamou, Y. Mébarki, A hybrid fuzzy logic proportional-integral-derivative and conventional on-off controller for morphing wing actuation using shape memory alloy, Part 1: Morphing system mechanisms and controller architecture design, *The Aeronautical Journal*, vol. **116**, no 1179, pp. 433-449, 2012.
- [35] T. L. Grigorie, A. V. Popov, R. M. Botez, M. Mamou, Y. Mébarki, A hybrid fuzzy logic proportional-integral-derivative and conventional on-off controller for morphing wing actuation using shape memory alloy Part 2: controller implementation and validation, *The Aeronautical Journal*, vol. **116**, no 1179, pp. 451- 465, 2012.
- [36] T. L. Grigorie, R. M. Botez, A. V., Popov, Chapter 1, *Fuzzy logic control of a smart actuation system in a morphing wing*, published in the book: *Fuzzy Controllers- Recent Advances in Theory and Applications*, ISBN 978-953-51-0759-0, INTECH, 22 pp., September 27, 2012.
- [37] T. L. Grigorie, R. M. Botez, Adaptive neuro-fuzzy inference system based controllers for smart material actuator modeling, Proceedings of the Institution of Mechanical Engineers, Part G., *Journal of Aerospace Engineering*, vol. **223**(G6), no 5, pp. 655-668, 2009.
- [38] R. Pecora, S. Barbarino, A. Concilio, L. Lecce, S. Russo, Design and Functional Test of a Morphing High-

- Lift Device for a Regional Aircraft, *Journal of Intelligent Material Systems and Structures*, Vol. **22**(10), pp. 1005-1023, 2011.
- [39] R. Pecora, F. Amoroso, L. Lecce, Effectiveness of Wing Twist Morphing in Roll Control, *Journal of Aircraft*, Vol. **49**(6), pp. 1666-1674, 2012.
- [40] R. Pecora, F. Amoroso, G. Amendola, A. Concilio, Validation of a smart structural concept for wing-flap camber morphing, *Smart Structures and Systems*, Vol. **14**(4), pp. 659-678, 2014.
- [41] R. Pecora, M. Magnifico, F. Amoroso, E. Monaco, Multi-parametric flutter analysis of a morphing wing trailing edge, *Aeronautical Journal*, Vol. **118**(1207), pp. 1063-1078, 2014.
- [42] S. Barbarino, R. Pecora, L. Lecce, A. Concillio, S. Ameduri, L. De Rosa, Airfoil structural morphing based on SMA actuator series: numerical and experimental studies, *Journal of Intelligent Material Systems and Structures*, Vol. **22**, pp. 987-1003, 2011.
- [43] H. E. Rauch, R. J. Kline Schoder, J. C. Adams, H. M. Youssef, Fault detection, isolation and reconfiguration for aircraft using neural networks, AIAA Paper 1993-3870, 1993.
- [44] D. J. Linse and R. F. Stengel, Identification of aerodynamic coefficients using computational neural networks, *Journal of Guidance, Control and Dynamics*, Vol. **16**(6), pp. 1018-1025, 1993.
- [45] R. Wallach, B. S. De Mattos, R. Da Mota Girardi, *Aerodynamic coefficient prediction of a general transport aircraft using neural network*, 25th International Congress of the Aeronautical Sciences ICAS, 2007.
- [46] A. Ben Mosbah, R. Botez, T. M. Dao, *New methodology for the calculation of aerodynamic coefficients on ATR-42 scaled model with neural network – EGD method*, ASME 2014 International Mechanical Engineering Congress and Exposition, November 14-20, Montreal, Que., Canada, 2014.
- [47] A. Ben Mosbah, R. Botez, T. M. Dao, *New methodology for calculating flight parameters with neural network, Extended Great Deluge method applied on a reduced scale wind tunnel model of an ATR-42 wing*, AIAA Aerospace Sciences – Flight Sciences and Information Systems Event, Boston, MA., – USA, 19 - 22 August, 2013.
- [48] A. Ben Mosbah, R. Botez, T. M. Dao, *New methodology for calculating flight parameters with neural network – EGD method*, AÉRO 13, 60th Aeronautics Conference and AGM, Toronto, Ont., Canada, 30 April - 2 May, 2013.
- [49] M. D. Johnson and K. Rokhsak, Using artificial neural network and self-organizing maps for detection of airframe icing, *Journal of Aircraft*, Vol. **38**(2), pp. 224-230, 2001.
- [50] R. Aykan, Kalman filter and neural network-based icing identification applied to A340 aircraft dynamics, *Aircraft Engineering and Aerospace Technology: An International Journal*, Vol. **77** (1), pp. 23-33, 2005.
- [51] M. D. Johnson and K. Rokhsaz, *Using artificial Neural networks and self-organizing maps for detection of airframe icing*, 2000 Atmospheric Flight Mechanics Conference, Paper AIAA-2000-4099, 2000.
- [52] M. R. Napolitano and M. Kincheloe, On-line learning neural network controllers for autopilot systems, *Journal of Guidance, Control and Dynamics*, Vol. **33**(6), pp. 1008-1015, 1995.
- [53] A. Ben Mosbah, M. Flores Salinas, R. Botez, T. M. Dao, *New Methodology for Wind Tunnel Calibration Using Neural Networks - EGD Approach*, *SAE International Journal of Aerospace*, Vol. **6**, No. 2, pp.761-766, 2013.